

Electronic supplementary information for

Chemical Design of High Performance SPR Biosensor Based on a Dielectric Nanoparticle Assembly Supported onto a Gold-Thin Film

Pier Berling,¹ Mathias Dolci,¹ Spyridon Zafeiratos,² Thomas Gehin,³ Cédric Leuvrey,¹ Céline Kiefer,¹ Déborah WAGNER,⁴ Fouzia Boulmedais,⁴ Benoit P. Pichon^{*,1,5}

¹ Université de Strasbourg, CNRS, Institut de Physique et Chimie des Matériaux de Strasbourg, UMR 7504, F-67000 Strasbourg, France

² Institut de Chimie et Procédés pour l'Energie, l'Environnement et la Santé, UMR 7515 du CNRS-UdS 25 Rue Becquerel, 67087 Strasbourg, France

³ Université de Lyon, Institut des Nanotechnologies de Lyon (INL) – UMR CNRS 5270, Ecole Centrale de Lyon, 36 Avenue Guy de Collongue, 69134 Ecully cedex, France

⁴ Université de Strasbourg, CNRS, Institut Charles Sadron, UPR 22, F-67034 Strasbourg Cedex 2, France

⁵ Institut Universitaire de France, 1 rue Descartes, 75231 Paris Cedex 05

Corresponding Authors

E-mail: benoit.pichon@unistra.fr

Tel: 0033 (0)3 88 10 71 33, Fax: 0033 (0)3 88 10 72 47

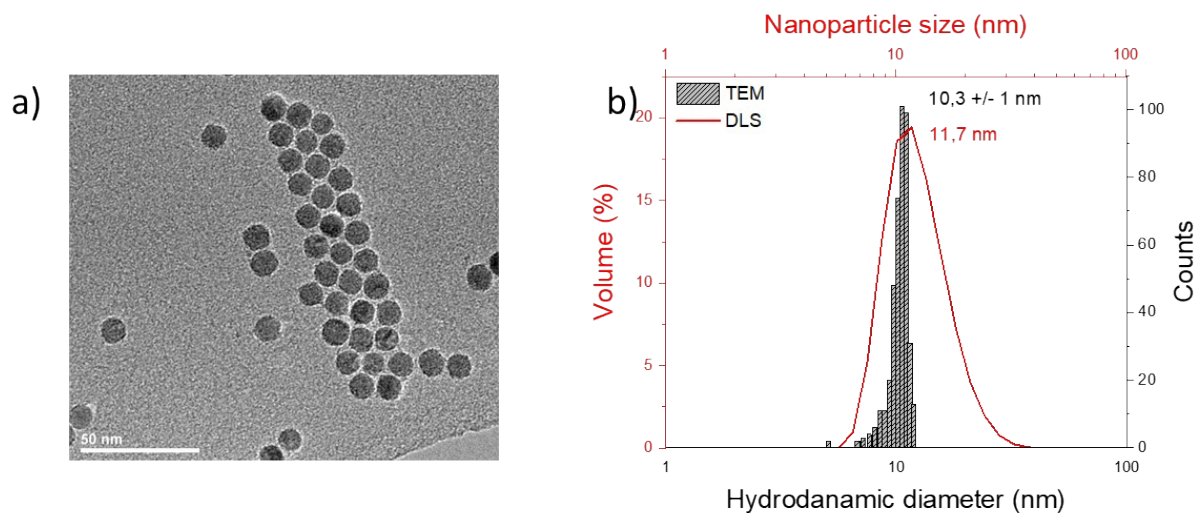


Figure S1. a) TEM micrographs of azide-terminated nanoparticles. b) The corresponding size distribution (histogram) and hydrodynamic diameter distribution (curve) obtained by granulometry measurement.

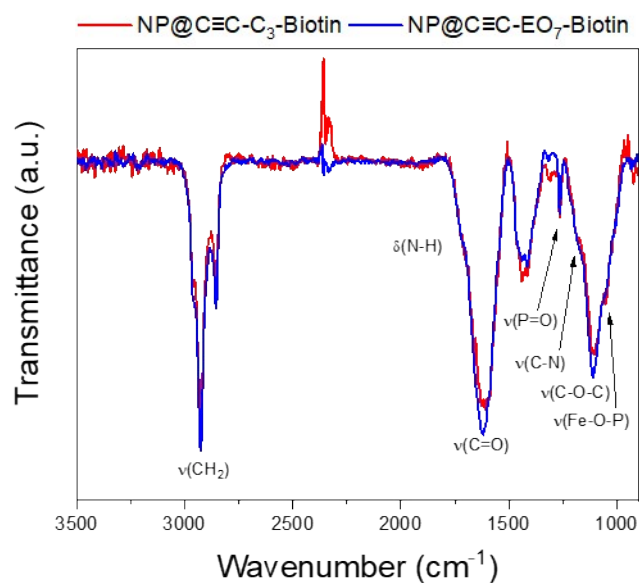


Figure S2. PM-IRRAS spectra of nanoparticle assemblies supported onto gold thin film and functionalized by C≡C-C3-Biotin and C≡C-EO7-Biotin.

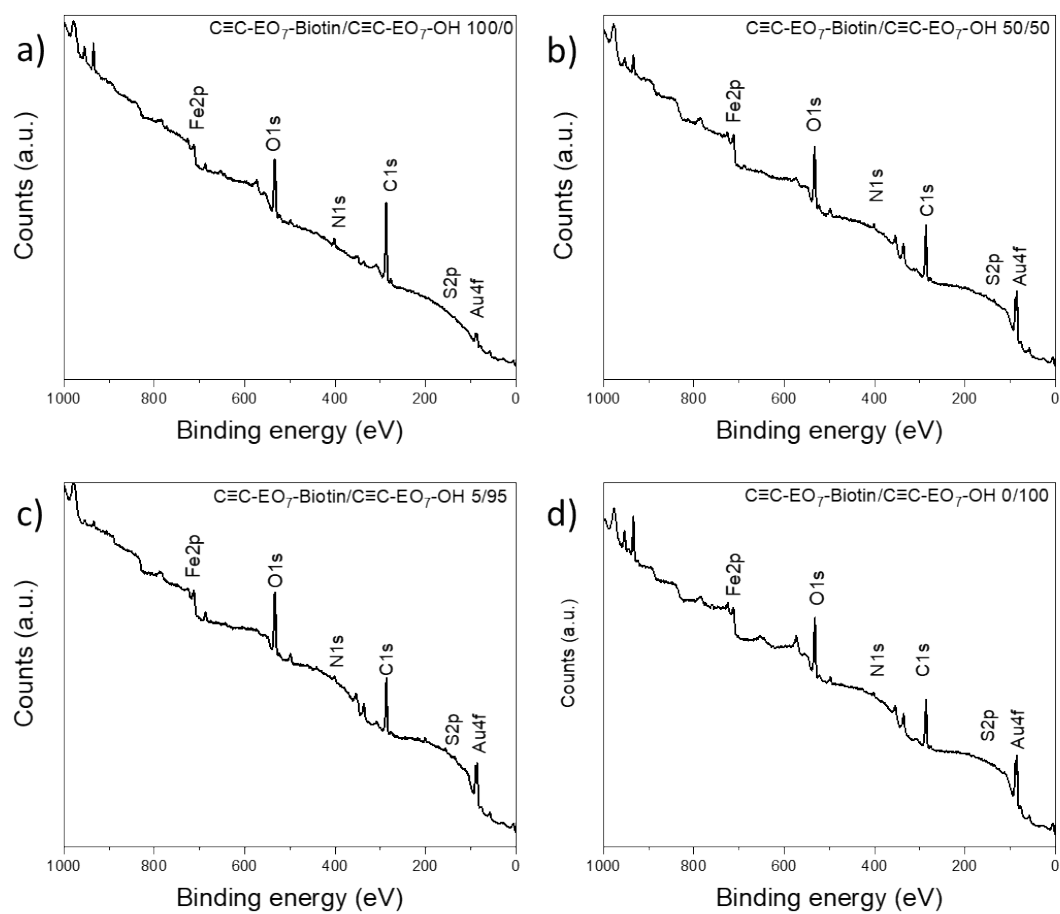


Figure S3. XPS: survey scan showing C_{1s}, O_{1s}, S_{2p}, Fe_{2p} signals for samples with various quantities of C≡C-EO₇-Biotin of a) 100%, b) 50 %, c) 5 %, d) 0%.

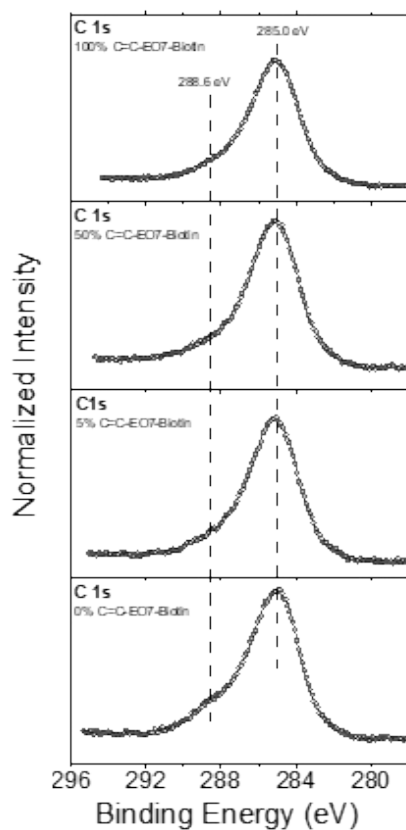


Figure S4. XPS spectra recorded in the C 1s region for samples after grafting different mol. % of C≡C-EO₇-Biotin at the surface of nanoparticle assemblies.

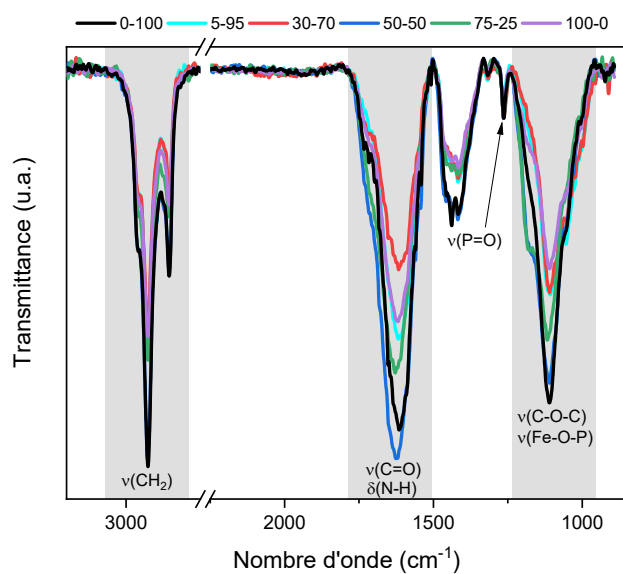


Figure S5. PM-IRRAS spectra of nanoparticle assemblies functionalized by mixtures of C≡C-EO₇-Biotin and PEO₇-N₃. Spectra were normalized to the a) νP=O band (1 255 cm⁻¹) and b) νC-H band (2922 cm⁻¹).

PM-IRRAS spectra recorded for all samples while lowering the C≡C-EO7-Biotin mol. % are very similar to 100 % C≡C-EO7-Biotin content, in agreement with PEO7 chains of the diluting agent. We can observe in both PM-IRRAS spectra the characteristic band of $\nu(\text{C-N})$ at $1\,180\text{ cm}^{-1}$ that increases with higher biotin concentrated samples. This band is more intense for 50/50 and 75/25 sample. We expected a similar intensity for 100/0 sample also, but we can observe a little shoulder in comparison to 5/95 and 30/70. The band corresponding to biotin at 1623 cm^{-1} ($\nu(\text{C=O})$) does not follow the percentages of biotin in the sample but slightly increases for the sample 50/50 and 75/25. The sample 30/70 is the one with the lowest $\nu(\text{C=O})$ intensity. Such inconstancies may be attributed to the different orientations of bonds in each sample because the measurement is performed by using polarized light.

Calculation of the decay length

The angular interrogation being performed at a fixed wavelength ($\lambda = 785\text{ nm}$), the decay length (l_d) only depends on the refractive index of the dielectric at the surface of the gold thin film:⁴⁰

$$l_d = \frac{\lambda}{2\pi} \sqrt{\left| \frac{\varepsilon_m + \varepsilon_d}{\varepsilon_d^2} \right|}$$

with ε_m and ε_d , the permittivity of the metal thin film and dielectric medium, respectively. ε is defined as \sqrt{n} .

After assembling of nanoparticles, the refractive index increases from 1.33 to 1.64 in the vicinity of the gold thin film surface. The refractive index corresponding to the nanoparticle assembly was calculated as a function of the volume fraction of iron oxide nanoparticles ($n_{\text{Fe}_3\text{O}_4} = 2.42$) in a layer with a thickness corresponding the size of nanoparticles. At a wavelength of 785 nm, l_d increases from 166 nm (gold thin film) to 204 nm (gold thin film with nanoparticles) which agree with other studies.⁴

Calculation of sensitivity factor m

Sensorgrams were recorded at 785 nm for samples which consist in a gold thin film (45 nm thick) uncovered or covered by iron oxide nanoparticles for several aqueous solutions of EtOH with concentrations (5 to 50 w/w%). Calibration curves corresponding to the position of the SPR peak were plotted against the refractive index (Figure S5). The sensitivity factor m corresponding to the slope increases after nanoparticle assembly onto the gold thin film (from $106.6 \pm 1.3^\circ/\text{RIU}$ to $114.2 \pm 2^\circ/\text{RIU}$), in agreement with previous studies.⁴

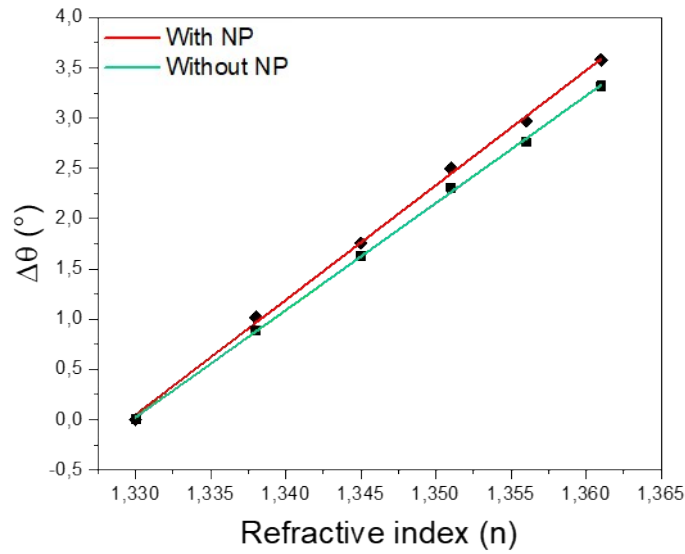


Figure S5. Calibration curves recorded at 785 nm for a gold thin film uncovered (green curve) and covered (red curve) by nanoparticles.

Calculation of the interparticle distance

The mean interparticle distance (D_{IP}) was calculated with the approximation that the nanoparticles are homogeneously distributed onto the surface of the gold thin film (Figure S7 a, b):¹⁴

$$D_{IP} = \sqrt{\frac{S}{N}} - D$$

with S the area considered for the density calculation (in our case, S will always be $1 \mu\text{m}^2 = 10^6 \text{ nm}^2$), N the number of nanoparticles on the surface S (determined by SEM) and D , the nanoparticle size.

Calculation of the available surface of nanoparticles to SA

The available surface area per nanoparticle to SA (S) was calculated according to:

$$S = \pi D \left(1 - \sin \left(\arccos \left(\frac{D - 4.5 + D_{IP}}{D} \right) \right) \right)$$

with D , the nanoparticle size with the organic layer and D_{IP} the inter-particle distance calculated as mentioned-above. S is then divided by the surface of a streptavidin (20.25 nm^2) to obtain the number of SA/NP (Figure S7c,d).

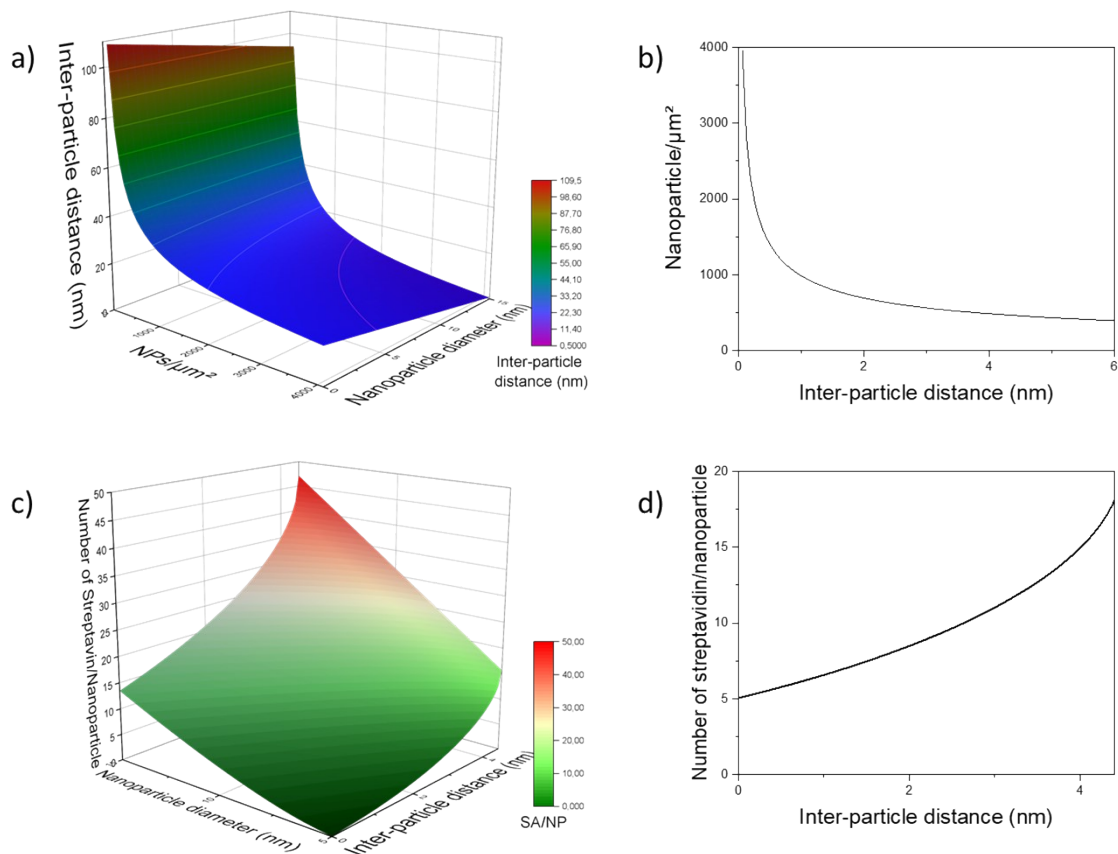


Figure S7. a) The inter-particles distance as a function of the size and the density is plot in 3D. b) The corresponding 2D plot for 10.3 nm sized nanoparticles. c) 3D plot of the number of streptavidin per nanoparticles as a function of the size of the nanoparticles and the inter-particle distance. d) The corresponding 2D plot for 10.3 nm sized nanoparticles.

Table S1. Mass concentration of SA ($\mu\text{g}/\text{mL}$) and the corresponding angular shift ($^\circ$), effective thickness of the adsorbate layer (t) and mass of SA.

| SA concentration ($\mu\text{g}/\text{mL}$) | SA concentration (nM) | $\Delta\theta$ ($^\circ$) | t (nm) | mass (ng/cm^2) |
|--|-----------------------|-----------------------------|----------|----------------------------------|
| 0.1 | 1,9 | 0,039 | 0,3 | 17 |
| 1 | 18 | 0,087 | 0,6 | 37 |
| 2.5 | 47 | 0,281 | 1,8 | 122 |
| 5 | 94 | 0,390 | 2,6 | 169 |
| 10 | 189 | 0,473 | 3,1 | 205 |